FINAL REPORT

Detection and Classification of Military Munitions Underwater Using Active Fluorometric Imaging (AFI)

ESTCP Project MR20-1472

Dr. Steven G. Ackleson
Dr. Robert J. Foster
Naval Research Laboratory

May 5, 2020

SERDP

REPORT DOCUMENTATION PAGE

Form Approved
OMB No. 0704-0188

1. REPORT DATE *(DD-MM-YYYY)*	2. REPORT TYPE	3. DATES COVERED *(From - To)*
05/05/2010	SERDP Final Report	

4. TITLE AND SUBTITLE

Detection and Classification of Military Munitions Underwater Using Active Fluorometric Imaging (AFI)

5a. CONTRACT NUMBER

5b. GRANT NUMBER

5c. PROGRAM ELEMENT NUMBER

6. AUTHOR(S)
Steven Ackleson
Robert Foster

5d. PROJECT NUMBER
MR20-1472

5e. TASK NUMBER

5f. WORK UNIT NUMBER

7. PERFORMING ORGANIZATION NAME(S) AND ADDRESS(ES)
Naval Research Laboratory
4555 Overlook Ave., SW
Washington, DC 20375

8. PERFORMING ORGANIZATION REPORT NUMBER
MR20-1472

9. SPONSORING/MONITORING AGENCY NAME(S) AND ADDRESS(ES)
Office of the Deputy Assistant Secretary of Defense (Energy Resilience & Optimization)
3500 Defense Pentagon, RM 5C646
Washington, DC 20301-3500

10. SPONSOR/MONITOR'S ACRONYM(S)
SERDP

11. SPONSOR/MONITOR'S REPORT NUMBER(S)
MR20-1472

12. DISTRIBUTION/AVAILABILITY STATEMENT

DISTRIBUTION STATEMENT A. Approved for public release: distribution unlimited.

13. SUPPLEMENTARY NOTES

14. ABSTRACT

This work addresses the objectives outlined in the FY 2022 SON in the Munitions Response Program Area, Detection, Classification, and Remediation of Military Munitions Underwater. The idea is that shallow water benthic features in natural environments, both biological and human constructed, often fluoresce when illuminated with blue light and that fluorescence signals contain information regarding objects of interest, such as obstacles to navigation and ordnance as well as marine organisms important for remediation efforts. The approach is referred to as Active Fluorescence Imaging (AFI), meaning that the imaging approach includes a dedicated illumination source to excite fluorescence and a sensor capable of recording the resulting fluorescence signals in high spectral resolution. In this initial laboratory test of the AFI concept, the light source is a dive light equipped with high intensity LEDs emitting at 464 nm and the sensor is a line imager that records the complete visible spectrum (400 – 720 nm) ay high spectral resolution (ECOTONE UHI; www.ecotone.com). The project objectives were to examine the sensitivity and noise attributes of the imager and to test the AFI approach within an experimental water tank under conditions of variable water clarity. The AFI concept is shown capable of imaging fluorescence from submerged targets through turbid water across attenuation lengths, defined as one-way transmission between the camera and target and measured at the illumination wavelength (464 nm), ranging between 2.8 (weak fluorescence) and 6.4 (strong fluorescence. Unlike reflectance signals, fluorescence is unaffected by path radiance (light backscattered by hydrosols), resulting in greater imaging distance and higher target contrast. A Monte Carlo radiative transfer model was developed to simulate the complete experimental setup. Model simulations are in excellent agreement with experimental results spanning a range in water turbidity serve to validate the AFI concept. The next step for the project is to configure the AFI components for deployment and testing in natural environments.

15. SUBJECT TERMS

UXO, target identification, active fluorometric imaging, AFI, system modeling

16. SECURITY CLASSIFICATION OF:			17. LIMITATION OF ABSTRACT	18. NUMBER OF PAGES	19a. NAME OF RESPONSIBLE PERSON
a. REPORT	b. ABSTRACT	c. THIS PAGE			Steven Ackleson
UNCLASS	UNCLASS	UNCLASS	UNCLASS	14	19b. TELEPHONE NUMBER *(Include area code)* 202-767-3398

FINAL REPORT

Project: MR20-1472

TABLE OF CONTENTS

LIST OF FIGURES

Detection and Classification of Military Munitions Underwater Using Active Fluorometric Imaging (AFI); MR20-1472

Final Report

May 5, 2020

Dr. Steven G. Ackleson, steve.ackleson@nrl.navy.mil, 202-767-3398

Dr. Robert J. Foster
Naval Research Laboratory, 4555 Overlook Ave., SW, Washington, D.C.

Abstract

This work addresses the objectives outlined in the FY 2022 SON in the Munitions Response Program Area, Detection, Classification, and Remediation of Military Munitions Underwater. The idea is that shallow water benthic features in natural environments, both biological and human constructed, often fluoresce when illuminated with blue light and that fluorescence signals contain information regarding objects of interest, such as obstacles to navigation and ordnance as well as marine organisms important for remediation efforts. The approach is referred to as Active Fluorescence Imaging (AFI), meaning that the imaging approach includes a dedicated illumination source to excite fluorescence and a sensor capable of recording the resulting fluorescence signals in high spectral resolution. In this initial laboratory test of the AFI concept, the light source is a dive light equipped with high intensity LEDs emitting at 464 nm and the sensor is a line imager that records the complete visible spectrum (400 – 720 nm) ay high spectral resolution (ECOTONE UHI; *www.ecotone.com*). The project objectives were to examine the sensitivity and noise attributes of the imager and to test the AFI approach within an experimental water tank under conditions of variable water clarity. The AFI concept is shown capable of imaging fluorescence from submerged targets through turbid water across attenuation lengths, defined as one-way transmission between the camera and target and measured at the illumination wavelength (464 nm), ranging between 2.8 (weak fluorescence) and 6.4 (strong fluorescence. Unlike reflectance signals, fluorescence is unaffected by path radiance (light backscattered by hydrosols), resulting in greater imaging distance and higher target contrast. A Monte Carlo radiative transfer model was developed to simulate the complete experimental set-up. Model simulations are in excellent agreement with experimental results spanning a range in water turbidity serve to validate the AFI concept. The next step for the project is to configure the AFI components for deployment and testing in natural environments.

Background

Optical imaging of benthic features underwater is a challenging problem due to the confounding effects of attenuation (the combination of absorption and light scatter) by the various substances dissolved and suspended within the water column. Absorption decreases light intensity (photon density) while scatter changes the direction of photon propagation. For an active system, e.g., one that produces the illumination energy, light must traverse the water column from the source to the object of interest with an associated attenuation factor proportional to $e^{-r(c)}$, where r is the geometric target distance (m) and c is the attenuation coefficient (m^{-1}). Imaging distance may also be described as attenuation lengths separating the sensor and target; $AL = r * c$. As the illumination energy propagates to the target, a portion of the light energy is scattered back to the sensor by particles suspended within the water. This backscattered energy, referred to as path radiance, does not contain information regarding benthic targets of interest, but is added to the received reflectance signal as a component of noise. The maximum target distance using traditional reflectance imaging is 2 to 3 *AL* (Jaffe et al., 2001).

AFI offers advantages over the traditional approach in that the signals of interest, spectral fluorescence, are unique and distinguishable from the associated reflectance signal and hydrosol scatter from the intervening water column. In the traditional approach, illumination at a specified wavelength, λ, is reflected from the benthic feature and the resulting image is formed at

the same wavelength. In the AFI approach, illumination photons are absorbed by the benthic feature and re-emitted at a longer wavelength, λ'. Thus, the received fluoresced radiance will form an image that 1) is free of path radiance, assuming no significant water column sources of fluorescence, and 2) contains spectral information about benthic features that is not included in reflectance.

The information content of benthic fluorescence is primarily the presence (or absence) of pigments, most of which are photosynthetic. However, some fluorescent pigments are associated with animals, such coral hosts, sponges, and pigments designed for natural camouflage. Macrophytic communities often have compositional, and therefore fluorescent, attributes that are affected by the substrate on which they are growing. Furthermore, aspects of man-made objects such as hydrocarbons associated with some benthic-mounted mines fluoresce and are spectrally unique from the naturally occurring benthic features (Jaffe et al., 2001). Thus, benthic objects can be detected by unique fluorescence characteristics, such as the epiphytic community, identifying markings and lubricants, and contrast (positive or negative) between an object of interest and the background environment.

AFI was illustrated in an Office of Naval Research Project (managed by Dr. Ackleson) over two decades ago using a multi-channel, synchronous laser imaging system that illuminated the sea floor at 488 nm and recorded fluorescent emissions at three wavelengths; 520 nm, 580 nm, and 685 nm (Strand et al., 1997, Mazel et al., 2003). The system was deployed on a coral reef and the imagery processed to detect inserted mine casings and map key ecological features with high accuracy (Fig. 1). It was discovered that non-fluorescent features embedded within the natural seascape were far more easily detected and identified due to the fluorescence contrast with the surrounding bottom. AFI images tend to be sharper, contain target information not present in reflectance imagery, and have the potential to image through longer path lengths of turbid water.

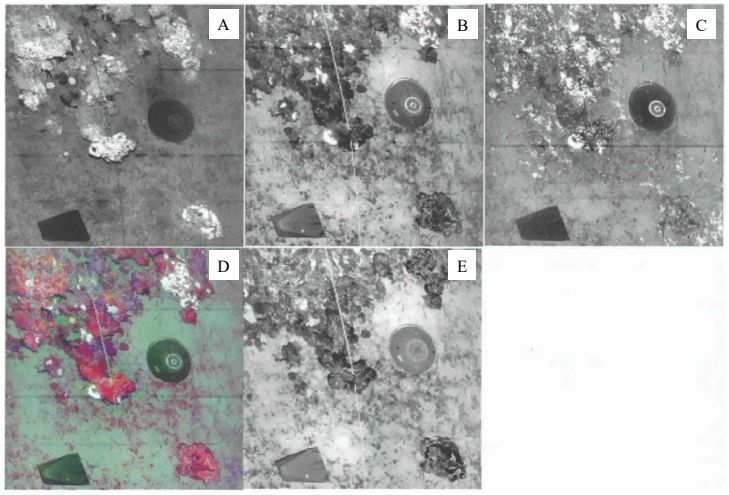

Figure 1. AFI of a coral reef and embedded mine-like objects produced with a multi-channel LLS system operating at 488 nm illumination. The top row (A – C), shows fluorescence images at 520, 580, and 685 nm emission wavelengths, respectively. The bottom left image (D) is a color composite of the fluorescence channels and the bottom right image (E) is reflectance at 488 nm.

An AFI approach need not include complicated imaging architectures, such as synchronous laser scanning. All that is necessary is that enough excitation energy propagate to the target and that the coupled sensor is capable of detecting the resulting fluorescence signals. In this project, we investigate the use of ultra-bright LEDs to provide excitation energy in the blue portion of the spectrum and a recently developed submersible line imager that records signals across the visible spectrum in high spectral resolution (ECOTONE UHI, *https://ecotone.com*). The goals of the project were to examine the sensitivity and noise attributes of

the UHI sensor and to test the AFI approach under controlled laboratory conditions. The results serve to demonstrate how AFI can potentially be used to survey shallow aquatic systems for natural and anthropogenic benthic features in shallow coastal environments with greater efficiency, less system complexity, and lower cost compared with traditional optical approaches.

Approach

The AFI concept is based on high-intensity blue LED illumination and fluorescence sensing in high spectral resolution. The UHI sensor is a submersible line imager equipped with a high-efficiency CMOS detector that records radiance across the visible spectrum (400 – 720 nm) in high spectral resolution ranging between 2.2 – 5.5 nm spectral band width (Fig. 2). The UHI records simultaneously in-water reflectance and fluorescence signals from targets of interest and yields spectral information that greatly exceeds the information content of broad-band detectors (Ludvigsen et al., 2014; Tegdan et al., 2015; Johnsen et al., 2016; Letnes et al., 2017). The test light source is a submersible LED dive light operating at 464 nm (Light and Motion, Sola Dive, *https://lightandmotion.com*). The Sola is a rechargeable light and the blue LED model was designed specifically to examine fluorescence from natural features in situ.

Ecotone Underwater Hyperspectral Imager

Specifications

Depth Rating:	3000 m
Frame Rate:	0.1–90 Hz
Field of View:	60°
Pixels per line:	1936
Spectral Range:	400–720 nm
Spectral Resolution:	2.2–5.5 nm
Exposure Time:	1–10000 ms

Light in Motion Sola Blue LED Dive Light

Depth Rating:	100 m
Output Wavelength:	464 nm
Output:	3000 mW
Beam Angle:	60°, 12°

Figure 2. AFI test components.

The AFI concept was tested in a 500 L water tank (Fig. 3). Water clarity was adjusted using quantities of Arizona Ultra-fine test dust (average particle diameter = 5 μm) and the sediment was kept in suspension using a vertically rotating drum equipped with small paddles. Reflectance and fluorescent targets were attached to the drum and the position of the drum could be adjusted along the tank axis, providing imaging distances (*r*) of between 0.5 and 1.5 m. For

the majority of the experiments r = 1.0 m. The drum was painted flat black to reduce reflected light in the tank and to provide maximum contrast between the test targets and the background.

The UHI and dive lamp were positioned statically at one end of the tank, positioned at the

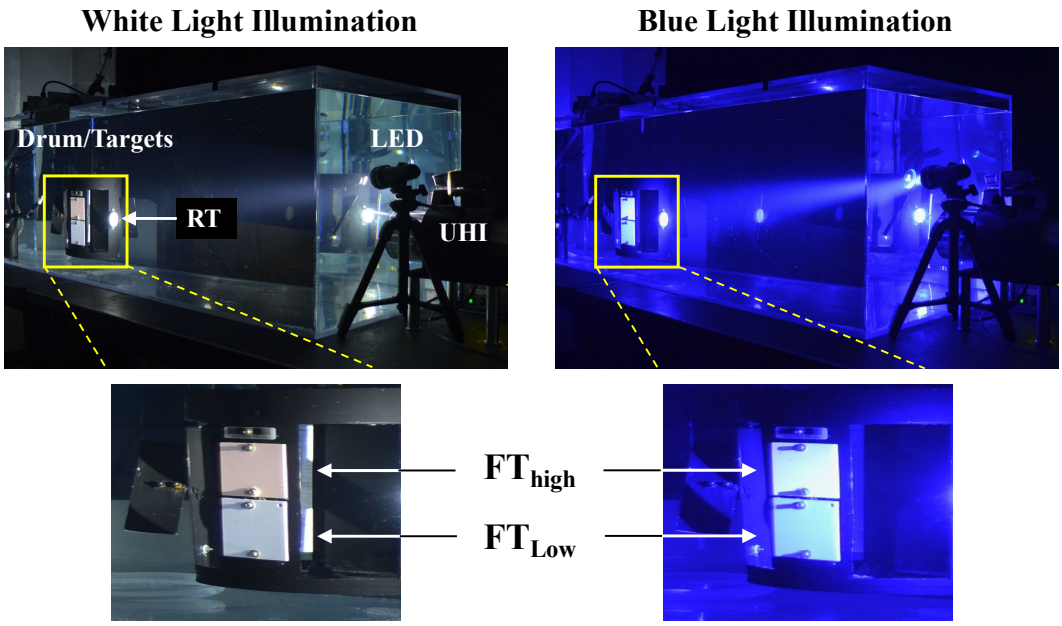

Figure 3. Experimental tank set-up.

outside face of the tank wall, and focused on the drum. The UHI imaging line was oriented vertically along the drum axis of rotation. In this configuration, targets fixed to the drum were moved across the imaging line as the drum rotated. The effect of the drum rotation was to simulate forward movement of the AFI system. Imagery consisted of the drum surface and attached targets repeating once per rotation. The drum rotation speed was adjustable to simulate forward speed of the AFI system. A spectral attenuation meter (Wet Labs ac-9) was positioned at the far end of the tank in order to monitor water clarity, expressed as c m^{-1}.

Three reflectance/fluorescence targets were considered; a 99% reflectance standard designed for underwater reflectance measurements (RT) and two fluorescence standards designed to bracket the fluorescence efficiencies (emission/illumination) of typical coral reef features; FT_{low} and FT_{high}, respectively. Target reflectance and fluorescence was measured prior to in-water experiments by imaging the targets through an empty tank (Fig. 4). Fluorescence efficiency was computed as

$$F_e = \frac{L_{ft}}{L_{rt}/0.99},$$

Where L_{ft} is the measured radiance from the fluorescence target and L_{rt} is the radiance from the 99% reflectance target. FT_{low} has a peak fluorescence efficiency of 0.4% at 538 nm while FT_{high}

has a peak efficiency of 4.8% at 497 nm. The targets are homogeneous in reflectance and fluorescence and provided a means to directly quantify the noise level of the UHI simply by measuring variability in target signal across each target, expressed as standard deviation, σ. Signal to noise ratio is expressed as $\bar{\omega}/\sigma$, where $\bar{\omega}$ is the mean target signal. Sensor noise is assumed dominated by shot noise and, therefore, σ is a function of signal intensity and proportional to $\sqrt{\bar{\omega}}$.

A typical experiment set-up consisted of positioning the drum 1 m from the UHI camera and light. Water attenuation was adjusted across a range of turbidity with additions of test dust. The clearest water condition consisted of tap water with no test dust added (c_{464} = 0.22 m^{-1}) and the most turbid condition resulted in c_{464} = 6.25 m^{-1}.

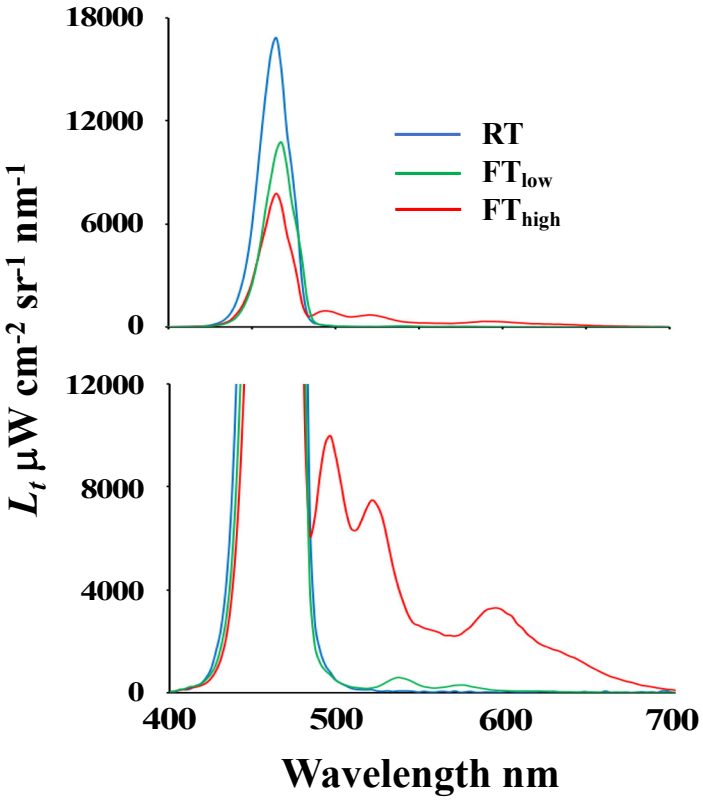

Figure 4. Target reflectance and fluorescence spectra measured with the AFI system in air.

In addition to laboratory experiments, the AFI concept was simulated using a 3-D Monte Carlo radiative transfer model, Coupled Land-Ocean Vector Rendering (CLOVER). The model includes a complete description of the AFI system components and the environment in which it is deployed, including water column optical properties, imaging distance, and the reflectance and fluorescence spectra of benthic targets and features (Fig. 5). The advantage of a Monte Carlo

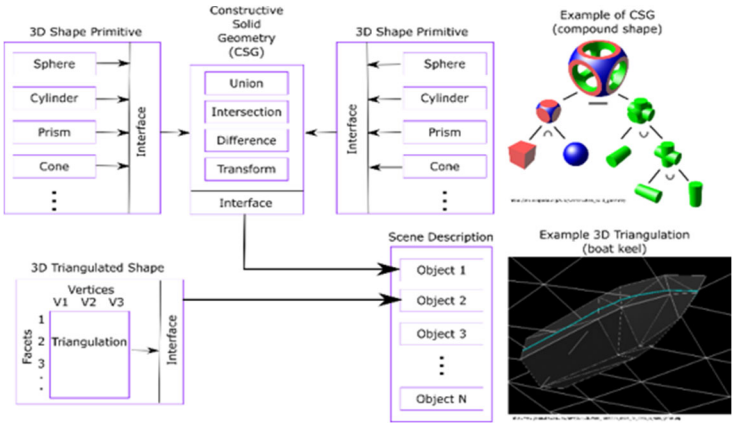

Figure 5. CLOVER Monte Carlo radiative transfer model configured to simulate the complete AFI experimental setup.

model is that it can simulate all possible scattering, reflection, and fluorescence events within the tank associated with targets, the tank walls, and the intervening water.

Results

The tank experiments indicate that the AFI approach is capable of detecting fluorescence signals across multiple attenuation lengths. The RT and FT_{low} targets are both detected at AL = 3.78 (Fig. 6). However, the FT_{high} signals are detected at a greater optical distance than either the RT

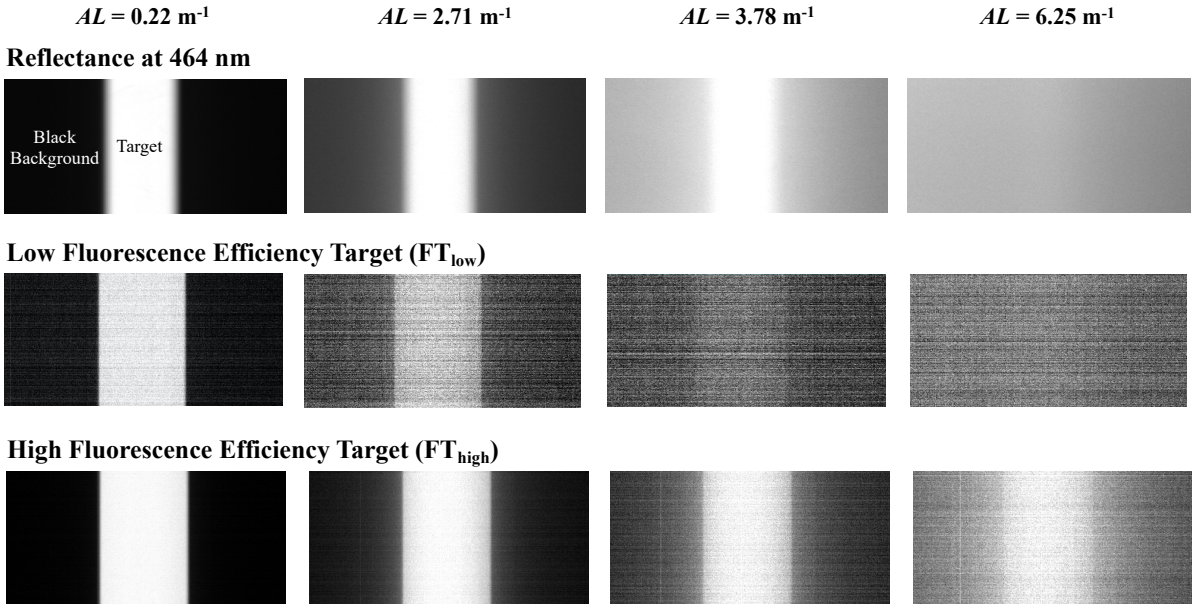

Figure 6. Selected results of AFI laboratory experiments. The targets were positioned 1 m from the UHI camera and LED light. The RT target is lower in contrast and the edges less sharp due to path radiance (top row) compared with the two fluorescence targets (middle and bottom rows). The high fluorescent target (bottom row) is apparent through nearly twice as many attenuation lengths as the reflectance and low fluorescence targets.

or FT_{low} signals; AL = 6.25. Additionally, since the fluorescence signals do not include path radiance the fluorescence images collected with elevated turbidity appear to have higher contrast compared with the reflectance imagery collected under the same water conditions.

The UHI is found to have high radiometric sensitivity coupled with low noise. For example, at the lowest gain setting, an integration time of 40 ms (maximum UHI integration time is 10,000 ms), and a received signal of 33 μW/(cm^2 sr nm), SNR = 25 (Fig. 7). This signal intensity is equivalent to the fluoresced light received from the FL_{high} target imaged through moderately turbid water, AL = 2.7. Increasing integration time will increase SNR, but at the cost of decreased target resolution in the forward direction, assuming that forward speed is held constant. Setting the integration time at 40 ms a forward platform speed of 0.4 m/s will result in an along-track sampling distance (spatial resolution) of 1.4 cm. Increasing integration time to 100 ms will increase the signal-to-noise, but the sampling distance in the along track direction will increase to 3.5 cm (decreased spatial resolution). Increasing along-track resolution with a longer integration time would require a slower platform speed and a proportional increase in the amount of time required to survey a given area.

To more quantitatively explore target contrast and edge sharpness, radiance signals were measured versus distance from the edge of each target (Fig. 8). Target contrast, C, is computed as

$$C = (\bar{L}_T - \bar{L}_B)/\bar{L}_B \,,$$

where the bar over each term indicates the average of all values measured outside of the edge effects and subscripts indicate target (T) and background (B). Target sharpness, S, is a measure of the geometric width of the transition region between target and background;

$$S = |P_{10} - P_{90}| \,,$$

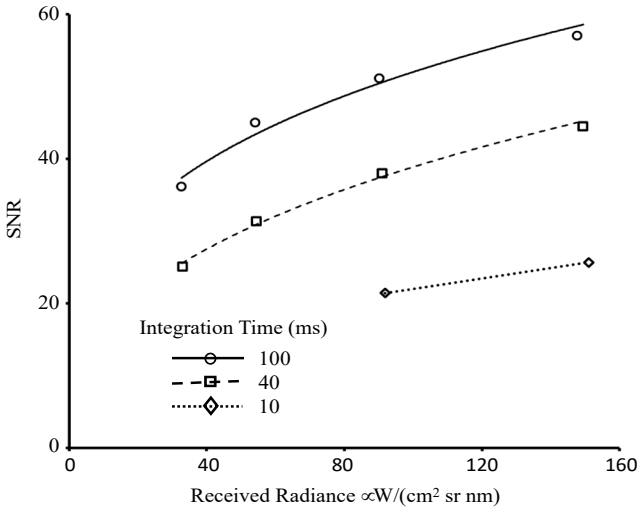

Figure 7. UHI sensor noise computed for integration times 100 ms (circles), 40 ms (squares), and 10 ms (diamonds).

where P is distance in micrometers from a reference position along a scan line and the subscripts 10 and 90 represent the percent change in radiance range between the target and background. Both the reflectance and fluorescence images result in sharp target edges when imaged through clear tap water. As turbidity increases, the transition in signal from target to background become less abrupt and S

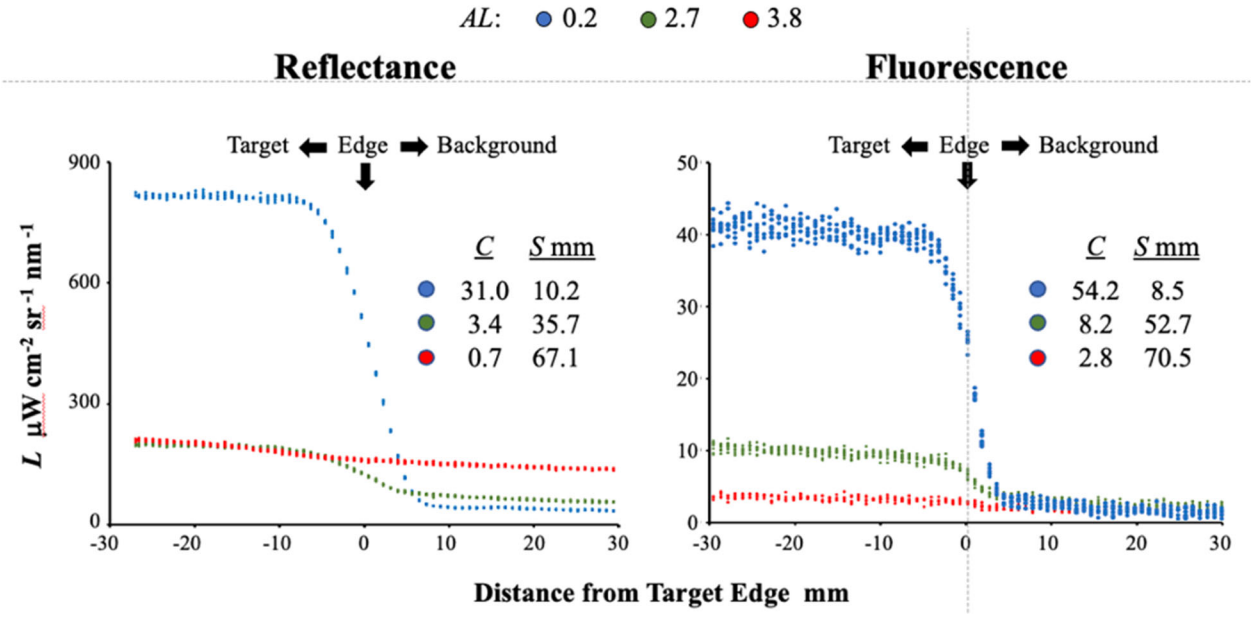

Figure 8. AFI target edge response as a function of turbidity; clear tap water (blue), low turbidity (green), and high turbidity (red). The reflectance target (RT) results are shown in the panel on the left and the high-efficiency fluorescent target (FT_{high}) results are shown in the panel on the to the right.

increases due to hydrosol scattering. This occurs with similar magnitude in both the reflectance and fluorescence images. Contrast, on the other hand, is significantly greater for the fluorescence targets compared with the reflectance target for each water turbidity level investigated. The difference is most pronounced for the target with high fluorescence efficiency, since the signal from the low efficiency fluorescence target is weaker and drops below the level of system noise for the highest turbidity investigated. The results from the reflectance target clearly show an increase in signal across the image domain with increasing turbidity. This is the effect of path radiance on image quality. However, the fluorescence signals, being outside of the illumination band, are not affected by path radiance as illustrated by the common minimum signal level representing the background of the image (right side of the fluorescence plots at distances greater that 10 mm from the target edge).

The radiative transfer model CLOVER reproduces the laboratory results in signal magnitude, contrast between targets and background, and the image blurring due to path radiance (Fig. 9). Under clear water conditions, the sharp demarcation between the target and the black drum background observed with the UHI, both reflectance and fluorescence, is accurately simulated with the model. Under high turbidity, blurring of the reflectance target by path radiance is also

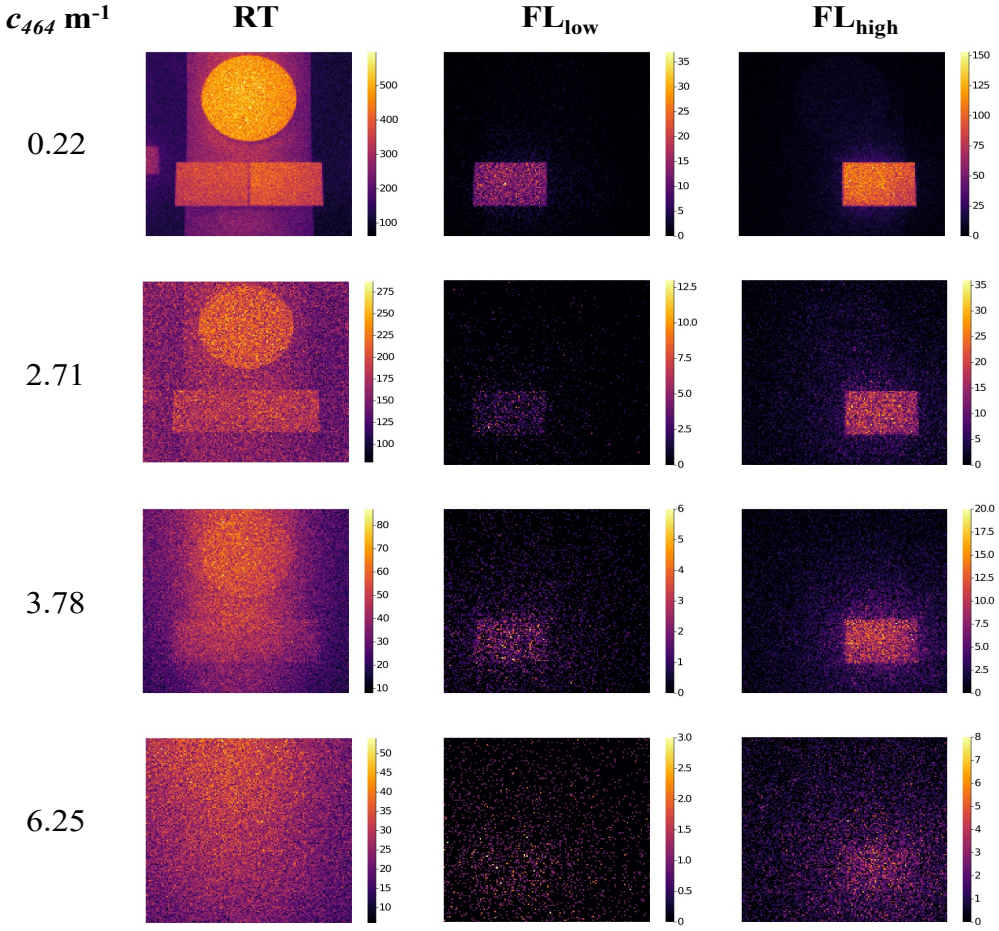

Figure 9. CLOVER simulations of laboratory experiments shown in Fig. 5; reflectance target (RT), low fluorescence target (FL_{low}), and high fluorescence target (FL_{high}). The color bars are photon counts received at the UHI sensor.

well captured as is the apparent contrast between target and background. Photon counts are higher for the RT scenarios because target reflectance is greater than light emissions from the fluorescence targets and, with increased turbidity, larger additions of path radiance in the illumination band. Also, in agreement with the experiment results, detection of the high fluorescence target is apparent at the highest turbidity while the reflectance target is indistinguishable from the background.

As with any photon-counting model, the life histories of many photons must be traced in order to converge on a statistically stable solution. This is achieved at the expense of time required to reach a solution. Typical CLOVER run-times were on the order of several hours. We expect that with future refinements of COVER towards greater efficiency, the model will continue to help guide the research and to aid in understanding the results. The excellent agreement between model runs and observations offer strong validation of the AFI approach.

Conclusion

The combination of a high-intensity, blue LED light source and a hyperspectral line imager is proved capable of imaging fluorescence from submerged targets through water with turbidity between 2.8 (weak fluorescence target) and 6.4 (strong fluorescence target) attenuation lengths, defined as one-way transmission between the camera and target and measured at the illumination wavelength (464 nm). Fluorescence returns are unaffected by path radiance, unlike reflected signals at the illumination wavelength, resulting in greater contrast between the target and background. For a highly fluorescent target, representing the upper bound of fluorescence efficiency found in natural benthic communities, the detection distance expressed as attenuation lengths is nearly twice the limit of a highly reflective target using traditional imaging methods. While reflectance imaging is ultimately limited by path radiance, AFI is only limited by the illumination intensity. If more photons that can be made to interact with the fluorescent material, then longer standoff range should be achievable resulting in higher SNR or faster survey speeds.

A Monte Carlo radiative transfer model, CLOVER, was developed to simulate the complete experimental set-up. Model simulations of individual experiments are in excellent agreement with observations spanning a range in water turbidity. The model provides helpful guidance in the project and aids in understanding the results. The excellent agreement between model runs and observations offer strong validation of the AFI approach.

The next logical step is to test the AFI concept in a variety of natural environments with realistic test targets and a range of water quality and stand-off distance. This will be an important step since the laboratory set-up did not permit imaging distances beyond 1.5 m. While the tank water turbidity could be adjusted, the associated attenuation length was dominated by light scatter from test particles. Water absorption, particularly at the blue illumination wavelength, was not a limiting factor. In natural environments, absorption due to the presence of colored dissolved organic matter (CDOM) from both terrestrial and marine sources increases significantly in the blue and UV portion of the spectrum, but has only minor influence on absorption in the green and red portions of the spectrum (Carder et al., 1989). Thus, natural CDOM is expected to attenuate the blue illumination energy as it propagates to benthic targets. While fluorescence return will not be impacted greatly by CDOM absorption, a reduction in excitation energy will result in a decrease in fluorescent emission. Quantifying this impact, increasing our knowledge of the spectral fluorescence attributes of natural and man-made targets, and understanding the limitations of AFI are best achieved with in situ tests in natural environments.

If the approach proves useful, we envision an AFI system configured for a small autonomous surface or sub-surface platform. While the current design oversamples the problem, allowing detailed investigations of spectral fluorescence from natural and human objects, a future operational system would likely not require hyperspectral signals. With better knowledge of the optimal emission bands, an operational system could be quite compact, relatively low-power, and include only a small number of high sensitivity detectors.

References

Carder, K. J., R. G. Steward, G. R. Harvey, and P. B. Ortner. Marine humic and fulvic acids: The effects in remote sensing of ocean chlorophyll. *Limnol. Oceanogr.*, 34(1), 68-81.

Jaffe, J. S., K. D. Moore, J. McLean, and M. P. Strand. 2001. Underwater optical imaging: Status and prospects. *Oceanography*, 14(3):64-75.

Johnsen, G., M. Ludvigsen, A. Sorensen, and L. M. S. Aas. 2016. The use of underwater hyperspectral imaging deployed on remotely operated vehicles – methods and applications. *IFAC-PapersOnLine*, 49-23:476-481.

Ludvigsen, M., G. Lohnsen, A. J. Sorensen, P. A. Lagstad, and O. Odegard. 2014. Scientific operations combining ROV and AUV in the Trondheim Fjord. *Mer. Tech. Soc. J.*, 48(2):59-71.

Letnes, P. A., et al. 2017. Underwater hyperspectral classification of deep-sea corals exposed to a toxic compound. *bioRxiv*, doi: 10.1101/150060.

Mazel, C. H., M. P. Strand, M. P. Lesser, M. P. Crosby, B. Coles, and A. J. Nevis. 2003. High resolution determination of coral reef bottom cover from multispectral fluorescence laser line scan imagery. *Limnol. Oceanogr.*, 48(1, part 23):522-534.

Strand, M. P., B. W. Coles, A. J. Nevis, and R. F. Regan. 1997. Laser line-scan fluorescence and multispectral imaging of coral reef environments. *SPIE*, Ocean Optics XIII, doi: 10.1117/12.266401.

Tegdan, J. et al. 2015. Underwater hyperspectral imaging for environmental mapping and monitoring of seabed habitats. *IEEE*, 978-1-4799-8736-8.